CrossMark

Discovery of an Isolated Dark Dwarf Galaxy in the Nearby Universe

Jin-Long Xu[1,2,3] ⓘ, Ming Zhu[1,2,3] ⓘ, Naiping Yu[1,2,3] ⓘ, Chuan-Peng Zhang[1,2,3] ⓘ, Xiao-Lan Liu[1,2,3] ⓘ, Mei Ai[1,2,3], and Peng Jiang[1,2,3]

[1] National Astronomical Observatories, Chinese Academy of Sciences, Beijing 100101, People's Republic of China; xujl@bao.ac.cn
[2] Guizhou Radio Astronomical Observatory, Guizhou University, Guiyang 550000, People's Republic of China; mz@nao.cas.cn
[3] CAS Key Laboratory of FAST, National Astronomical Observatories, Chinese Academy of Sciences, Beijing 100101, People's Republic of China

Abstract

Based on a new H I survey using the Five-hundred-meter Aperture Spherical radio Telescope (FAST), combined with the Pan-STARRS1 images, we identified an isolated H I cloud without any optical counterpart, named FAST J0139+4328. The newly discovered H I cloud appears to be a typical disk galaxy since it has a double-peak shape in the global H I profile and an S-like rotation structure in the velocity-position diagram. Moreover, this disk galaxy has an extremely low absolute magnitude ($M_B > -10.0$ mag) and stellar mass ($< 6.9 \times 10^5 M_\odot$). Furthermore, we obtained that the H I mass of this galaxy is $(8.3 \pm 1.7) \times 10^7 M_\odot$, and the dynamical mass to total baryonic mass ratio is 47 ± 27, implying that dark matter dominates over baryons in FAST J0139+4328. These findings provide observational evidence that FAST J0139+4328 is an isolated dark dwarf galaxy with a redshift of $z = 0.0083$. This is the first time that an isolated dark galaxy has been detected in the nearby universe.

Unified Astronomy Thesaurus concepts: Extragalactic astronomy (506)

1. Introduction

One of the puzzles in extragalactic astronomy is the disparity between the Λ cold dark matter (ΛCDM) predictions and observations of dwarf galaxy numbers (Kauffmann et al. 1993; Tollerud et al. 2008). It is also often referred to as the "missing satellite problem" (Moore et al. 1999). With the detection of a large number of dwarf galaxies and the improvement of theoretical models, the disparity has significantly decreased, and even this is no longer a missing satellite problem (Sales et al. 2022). However, the number of ultra-faint galaxies ($M_* < 10^5 M_\odot$) remains largely unconstrained (Bullock & Boylan-Kolchin 2017; Sales et al. 2022). For more massive galaxies, the various numerical simulations indicated a tight relation between halo mass and stellar mass with little scatter (Behroozi et al. 2013; Sawala et al. 2016). This relation did not hold true for ultra-faint galaxies, because the scatter was predicted to be greater. It indicates that a significant amount of theoretical uncertainty still exists. On the other side, a significant number of ultra-faint galaxies have not been detected in observations. Therefore, determining whether theoretical predictions and observations are consistent remains difficult. Dark galaxies are thought to be dark matter haloes whose gas failed to form stars (Roman et al. 2021). The existence of dark galaxies could offer a standard way to explain the problem of the absence of ultra-faint galaxies. Furthermore, the discovery of dark galaxies is crucial to understanding galaxy formation since gas-rich dark galaxies may reflect the earliest stage of galaxy formation.

The search for dark galaxies has been going on for many years, but none of the candidates appear to be ideal (Taylor et al. 2016). The southwestern (SW) clump of HI 1225+01 and the VIRGOHI 21 in the Virgo cluster are the best dark-galaxy candidates. However, both these candidates are just located at

the tidal tails, for which they could be considered as possible tidal debris (Turner & MacFadyen 1997; Duc & Bournaud 2008). Because it is difficult to determine whether the detected candidates are dark galaxies or just unusual tidal debris, the ideal candidates for a dark galaxy should be located far away from other massive galaxies, groups, and clusters. Blind neutral hydrogen (H I) surveys are one of the most efficient methods for searching dark galaxies. However, both the H I Parkes All Sky Survey (HIPASS) and Arecibo Legacy Fast ALFA (ALFALFA) surveys failed to find any isolated dark galaxies (Doyle et al. 2005; Haynes et al. 2011). Some previously discovered candidates were later found to be only a few almost dark galaxies based on deeper optical observations (Ball et al. 2018; Leisman et al. 2021). Davies et al. (2006) predicted that dark galaxies exist, but a significant portion of these galaxies may have masses less than $10^7 M_\odot$ and velocity widths under 40 km s^{-1}. Thus, both high sensitivity and high-velocity resolution play a key role in searching for dark galaxies in a new H I survey.

Using the Five-hundred-meter Aperture Spherical radio Telescope (FAST; Jiang et al. 2019, 2020), we set out to carry out a FAST extragalactic H I survey, which is a time-filler project when there are no other programs in the FAST observing queue. A major scientific objective for this survey is to search for dark and weak galaxies taking advantage of the high sensitivity of FAST and a relatively high-velocity resolution. In this Letter, based on the H I survey using FAST, we have discovered an isolated dark dwarf galaxy in the nearby universe.

2. Observation and Data Processing

For a new H I survey using FAST, the 19 beam array receiver system in dual polarization mode is used as the front end. It formally works in the frequency range from 1050 to 1450 MHz. For the backend, we choose the Spec(W) spectrometer that has 65,536 channels covering a bandwidth of 500 MHz for each polarization and beam, resulting in a
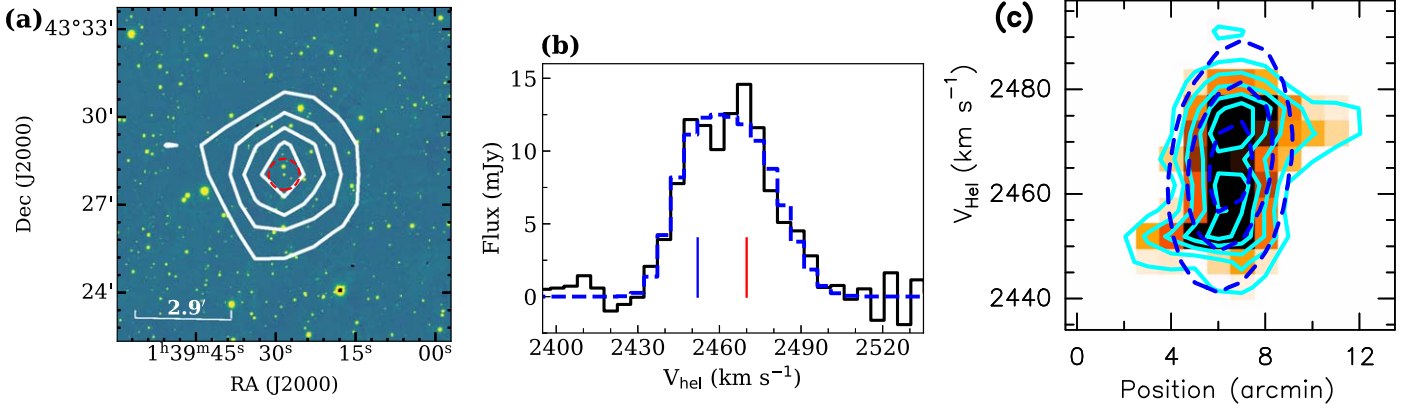
Figure 1. Morphology of dark galaxy FAST J0139+4328. (a) H I column-density map from the FAST observation shown in white contours overlaid on the Pan-STARRS1 g-band image in color scale. The white contours begin at 3.0×10^{18} cm^{-2} (3σ) in steps of 1.9×10^{18} cm^{-2}. The red dashed circle represents three times the expected D_{25}. (b) the global H I profile of FAST J0139+4328. The blue dashed line indicates the BusyFit fitting result. The red and blue vertical lines mark the positions of the double peak. (c) position–velocity (PV) diagram in color scale overlaid with the cyan contours. The cyan contours begin at 2σ (1.8 mJy beam^{-1}) in steps of 1σ. The blue dashed contours represent the PV diagram from the TiRiFiC fitting.

frequency resolution of 7.629 kHz and corresponding to a velocity resolution of 1.6 km s^{-1} at $z = 0$. The FAST H I survey uses the drift scan mode. An interval between two adjacent parallel scans in decl. is $\sim 1'.14$. Besides, we set an integration time of 1 s per spectrum. The system temperature was around 25 K. For intensity calibration to antenna temperature (T_A), a noises signal with an amplitude of 10 K was injected for 1 s every 32 s. The half-power beamwidth (HPBW) is $\sim 2'.9$ at 1.4 GHz for each beam. The pointing accuracy of the telescope was better than $10''$. The FAST H I observations of FAST J0139+4328 in the new survey were carried out on 2021 August 2 (region ID: DEC+433059-6). The detailed data reduction is similar to Xu et al. (2021). According to Zhang et al. (2022), we flag radio frequency interferences (RFIs). The RFI contamination rate is minimal in the FAST data used in this paper. The beamwidth after gridding is $\sim 3'.1$. A gain T_A/S_v has been measured to be about 16 K Jy^{-1}. The measured relevant main beam gain T_B/S_v is about 21 K Jy^{-1} at 1.4 GHz for each beam, where T_B is the brightness temperature. To construct a highly sensitive H I image, the velocity resolution of the FAST data is smoothed to 4.8 km s^{-1}. The mean noise rms in the observed image is ~ 0.9 mJy beam^{-1}.

3. Results

So far, we have detected some new H I clouds in the local universe based on the new FAST extragalactic H I survey data. Among these detected clouds, we found an isolated cloud, named FAST J0139+4328 according to its coordinates. The isolated clouds are typically thought to have no relatively massive galaxies within a radius of 100 kpc (Taylor et al. 2017). Under the assumption that the gas in galaxies is optically thin for the H I line, the column density $N(x, y)$ in each pixel can be estimated as $N(x, y) = 1.82 \times 10^{18} \int T_B dv$, where dv is the velocity width in km s^{-1}. Figure 1(a) shows the H I column-density map of FAST J0139+4328, overlaid on the Pan-STARRS1 g-band image in color scale. From the H I emission, we can see that FAST J0139+4328 has a compact structure. In Figure 1(b), we display the global H I profile of FAST J0139+4328. The H I profile seems to exhibit a double-peak shape, which is generally thought to be caused by the flat rotation curve of a disk galaxy. We performed a BusyFit fitting

Table 1
Measured and Derived Properties of Dark Galaxy FAST J0139+4328

Name	FAST J0139+4328
R.A.	$01^h39^m28^s.4$
Decl.	$43° 28'02''.6$
W_{50} (km s^{-1})	38.9 ± 1.9
W_{20} (km s^{-1})	51.1 ± 2.0
V_{sys} (km s^{-1})	2464.4 ± 0.8
D (Mpc)	28.8 ± 2.9
R_{eff} (kpc)	23.9 ± 2.4
i (deg)	27.0 ± 11.6
PA (deg)	151.0 ± 3.0
V_{rot} (km s^{-1})	26.9 ± 9.4
σ_v (km s^{-1})	7.8 ± 1.4
M_{II} ($M_\odot$)	$(8.3 \pm 1.7) \times 10^7$
M_{dyn} ($M_\odot$)	$(5.1 \pm 2.8) \times 10^9$
$E(B - V)$	0.08
m_g (mag)	>22.0
m_r (mag)	>21.7
m_B (mag)	>22.4
M_g (mag)	>-10.3
M_r (mag)	>-10.7
M_B (mag)	>-10.0
L_B ($L_\odot$)	$<1.4 \times 10^6$
$M_\star$ ($M_\odot$)	$<6.9 \times 10^5$

Note. We list: equatorial coordinates (R.A., Decl.); line widths at 50% of the peak flux (W_{50}); line widths at 20% of the peak flux (W_{20}); system velocity (V_{sys}); distance (D); effective radius (R_{eff}); inclination angle (i); position angle (PA); rotation velocity (V_{rot}); velocity dispersion (σ_v); H I gas mass (M_{II}); dynamic mass (M_{dyn}); reddening ($E(B - V)$); g-band, r-band, and B-band apparent magnitudes (m_g, m_r, m_B), which are corrected for Galactic extinction; absolute g-band, r-band, and B-band magnitudes (M_g, M_r, M_B); B-band luminosity (L_B); stellar mass ($M_\star$).

to the profile to determine the system velocity (V_{sys}), total flux (S_v), and line widths at 50% of the peak flux (W_{50}) and at 20% of the peak flux (W_{20}). The busy function is a new analytic function for describing the integrated H I spectral profile of galaxies (Westmeier et al. 2014). The parameters obtained by the fitting are listed in Table 1.

Figure 1(c) shows the position–velocity (PV) diagram in cyan contours for FAST J0139+4328. The extracted PV diagram passes through the center of FAST J0139+4328 with a

length of $14'.0$ along a position angle of $151°$. From the PV diagram, we see that FAST J0139+4328 seems to have two velocity components, which are associated with the double-peak shape in its global H I profile. In addition, the whole PV diagram displays an S-like structure, which is a typical characteristic of disk galaxies. Based on the presence of the global H I profile, and S-like rotation structure, we suggest that the H I cloud FAST J0139+4328 is a newly discovered disk galaxy. Gas in galaxies mainly consists of H I and helium. The H I gas mass of FAST J0139+4328 can be estimated as $M_{II} = 2.36 \times 10^5 D^2 \int S_\nu dv$, where $\int S_\nu dv$ is the integrated H I flux in Jy km s^{-1}, and D is the adopted distance in Mpc to FAST J0139+4328. We derived that the total S_ν is 424 ± 20 mJy km s^{-1} from the global H I profile of FAST J0139+4328, and the system velocity V_{sys} is 2464.4 ± 0.8 km s^{-1}, corresponding to redshift $z = 0.0083$. Using the Cosmicflows-3 method (Kourkchi et al. 2020), the distance to FAST J0139+4328 can be estimated to be 28.8 ± 2.9 Mpc. Finally, for FAST J0139+4328, we obtained that M_{II} is $(8.3 \pm 1.7) \times 10^7 M_\odot$.

The Pan-STARRS1 survey is a 3π steradian survey with a medium depth in five bands (Chambers et al. 2016). To investigate the presence of stellar components that could be associated with galaxy FAST J0139+4328, we use the Pan-STARRS1 r-band and g-band archive images. Figure 1(a) shows the Pan-STARRS1 g-band mosaic image in color scale. Interestingly, we have not detected any extended optical emission in the H I plane of this galaxy. But we can make some restrictions on the results of the optical observation. Previous work on galaxies discovered a tight relation between the H I mass (M_{HI}) and the optical disk diameter (D_{25}): log $_{10}(M_{HI}) = a + b \times$ log $_{10}(D_{25})$, where D_{25} is measured at 25 mag arcsec^{-2} level in B band (Solanes et al. 1996; Broeils & Rhee 1997; Toribio et al. 2011). The coefficients for normal spiral galaxies can be adopted as $a = 7.0$ and $b = 1.95$ (Broeils & Rhee 1997). Using the obtained M_{HI}, we expect the D_{25} value to be ~ 2.9 kpc $(21'')$ for FAST J0139+4328. Figure 2(a) shows a zoomed-in image in the Pan-STARRS1 g band, which is three times the expected D_{25} size, as indicated by the red dashed circle. The Gaia data can provide the most precise parallaxes for the identified stars. Through the parallax, we can obtain the relatively accurate distance of these stars. Using the Gaia source catalog (Gaia Collaboration et al. 2016), we identified five bright stars, which are marked in black dashed circles. Among these stars, the farthest one with a parallax distance of ~ 13 kpc is located within the predicted D_{25} region. As a result, we were able to confirm that the bright stars in the zoomed-in image are some Galaxy stars. Yet we have not detected an optical counterpart for galaxy FAST J0139+4328. The 2MASS K-band and GALEX near-ultraviolet (NUV)-band images are often used to determine whether there has been any new star formation recently (Martin et al. 2005; Skrutskie et al. 2006). We also did not detect any sign of star formation in galaxy FAST J0139+4328 based on the images in Figures 2(b) and (c).

Furthermore, strong L-band emission without an optical counterpart is detected as those of radio recombination lines (RRL) from a Galaxy H II region (Zhang et al. 2021) or OH megamasers from a luminous/ultra-luminous infrared galaxy (Zhang et al. 2014; Hess et al. 2021; Glowacki et al. 2022). However, using the Simbad and NED database, we are unable to locate an infrared galaxy in the three times the expected D_{25}

region. We also did not identify a luminous infrared galaxy in the WISE W4 image, as shown in Figure 2(d). Hence, we exclude the possibility that FAST J0139+4328 is an OH megamaser emission from a luminous infrared galaxy. In addition, if the identified FAST J0139+4328 is an H II region, we should be able to detect the radio continuous emission and UV emission. From the NRAO VLA Sky Survey (NVSS) archived images and UV image in Figure 2(c), we did not detect the corresponding emission. Moreover, the central frequency of this detection line in FAST J0139+4328 is about 1419.626 MHz. H166α is the radio recombination line closest to this signal, and its rest frequency is 1424.734 MHz. The frequency difference between FAST J0139+4328 and H166α is 5.108 MHz, corresponding to a velocity difference of about 1070 km s^{-1}, indicating that this detection line does not correspond to a Galactic redshift H II region. Hence we rule out the possibility that FAST J0139+4328 is some RRL emission from an H II region. Since no counterpart of RRL or OH megamaser emission is identified in this region, we suggest that FAST J0139+4328 is likely to be an isolated dark galaxy.

4. Discussion and Conclusion

The baryonic mass (M_{bar}) of the dark galaxy FAST J0139+4328 can be calculated using $M_{bar} = M_\star + M_{gas}$, where M_{gas} is the total gas mass. We do not consider the contribution of stellar mass $(M_\star)$ to baryonic mass for the galaxy FAST J0139+4328 because it does not have an optical counterpart. Assuming the same helium-to-H I ratio as that derived from the big bang nucleosynthesis, a factor of 1.33 is included to account for the contribution of helium. The total gas mass is determined with $M_{gas} = 1.33 \times M_{HI}$. We calculated the M_{bar} of FAST J0139+4328 to be $(1.1 \pm 0.3) \times 10^8 M_\odot$, indicating that FAST J0139+4328 could be a gas-rich dwarf galaxy. While the dynamic mass of galaxies can be estimated with $M_{dyn} = (V_{rot}^2 + 3\sigma_\nu^2) R_{eff}/G$ (Hoffman et al. 1996), where V_{rot} is rotation velocity, σ_ν is velocity dispersion, R_{eff} is the effective radius, and G is the gravitational constant. To correct for beam smearing effects, the effective radius can be calculated with $R_{eff} = \sqrt{S_F^2 - B_F^2}/2$, where B_F is the gridded beam size $(3'.1)$, and S_F is the uncorrected H I sizes of galaxies. We adopt the outmost size at 3σ level as S_F for FAST J0139+4328 from Figure 1(c). The obtained R_{eff} is 23.9 ± 2.4 kpc, which appears to be close to the scale of our Galaxy.

To estimate the V_{rot} of FAST J0139+4328, we use the Tilted Ring Fitting Code (TiRiFiC) software package to fit the observed H I cube data. The TiRiFiC is a freely available 3D tilted-ring fitting code (Józsa et al. 2007), which is a very successful approach to describing the kinematics and morphology of rotating disks. The bootstrap method is used to estimate the final values and errors of model parameters, which are listed in Table 1. We also derived the model cube data. In Figure 1(c), we show the PV diagram from the TiRiFiC model data for FAST J0139+4328 in the blue dashed contours. Through comparison, it shows that our model can construct the dynamic structure of FAST J0139+4328, except for the weak flat components. Using the fitted V_{rot} and σ_ν, we calculated that M_{dyn} is $(5.1 \pm 2.8) \times 10^9 M_\odot$, which is 47 ± 27 times its baryonic masses, implying that FAST J0139+4328 is dominated by dark matter within the error range. Here, due to the low resolution of the FAST, we can only roughly estimate the content of dark matter. In the near future, we will apply for the higher-angle resolution observation for FAST J0139+4328.
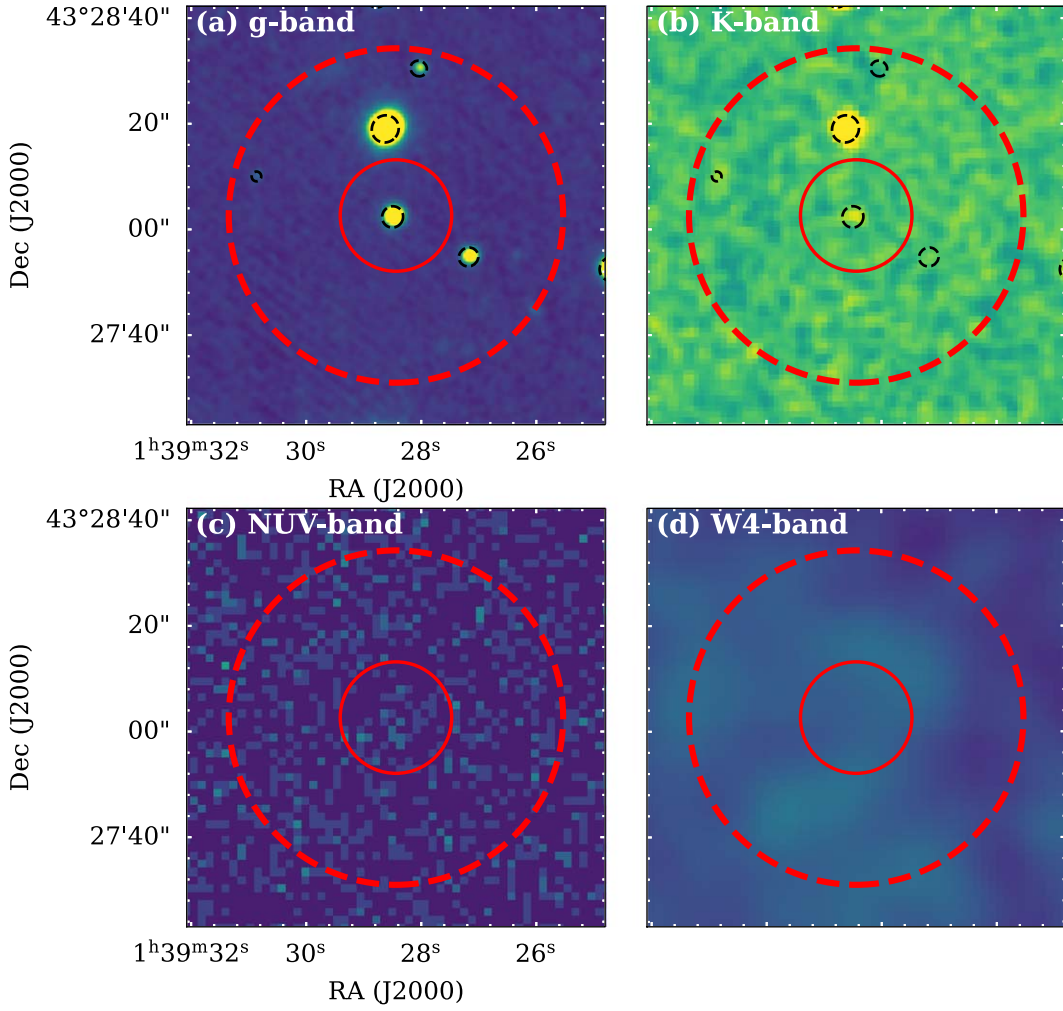
Figure 2. Images of dark galaxy FAST J0139+4328 in different bands. (a) Optical emission from the Pan-STARRS1 *g*-band data. (b) Near-infrared *K*-band emission from the 2MASS data. (c) Near-ultraviolet (NUV) emission from the GALEX data. (d) Mid-infrared emission (W4, 22 μm) from the WISE data. Fluxes in each band are on an arbitrary unit. The red solid and dashed circles represent the expected D_{25} and the three times D_{25} in each panel, respectively. The black ellipses mark optical stars in the Galaxy identified from the Gaia star catalog.
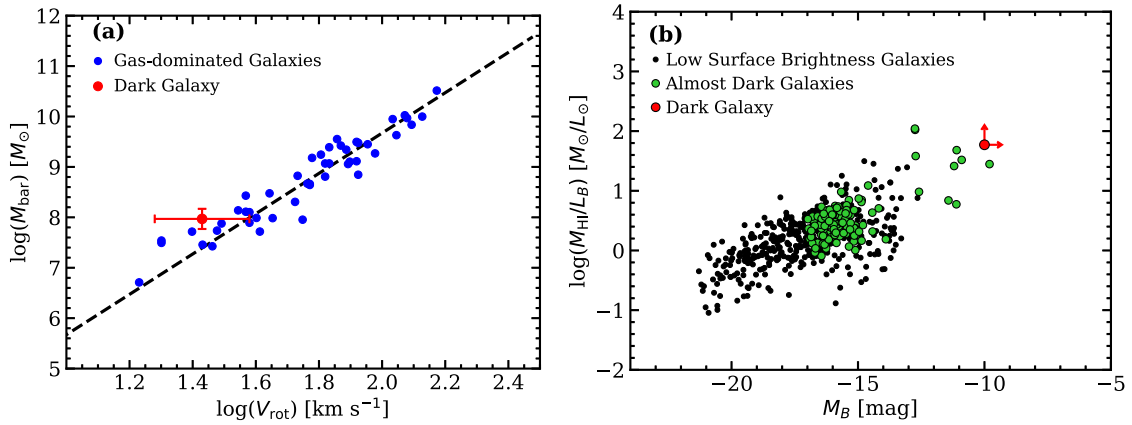
Figure 3. (a) Baryonic Tully–Fisher relation (BTFR). The black dashed line represents a best-fit relation $M_{bar} = A V_{rot}^4$ with $A = 47 \pm 6\, M_\odot \mathrm{km}^{-4}\mathrm{s}^4$, and gas-dominated galaxies are marked by black points (McGaugh 2012). The red point represents the discovered dark galaxy FAST J0139+4328. (b) Relation between the H I mass-to-light ratio and absolute *B*-band magnitude. The low surface brightness galaxies are obtained from Honey et al. (2018), while almost dark galaxies from Cannon et al. (2015), Janowiecki et al. (2015), Brunker et al. (2019), and Leisman et al. (2017), Leisman et al. (2021).

The Baryonic Tully–Fisher relation (BTF) is one of the strongest empirical correlations for disk galaxies. FAST J0139 +4328 has no optical counterpart, suggesting that it is gas dominated. We used the BTF to explore the properties of this

special galaxy. There is a best-fit relation $M_{bar} = A V_{rot}^4$ with $A = 47 \pm 6\, M_\odot\, \mathrm{km}^{-4}\mathrm{s}^4$ for gas-dominated disk galaxies (McGaugh 2012). Figure 3(a) shows the location of FAST J0139+4328 on the BTF relation. When compared to other

gas-dominated galaxies, FAST J0139+4328 nearly follows the best-fit relation, implying that this galaxy is also a normal disk galaxy. Nevertheless, the disk galaxy FAST J0139+4328 has no optical counterpart, so the internal extinction from dust should be relatively minimal. We can rule out the possibility that internal extinction is the cause of the absence of an optical counterpart. Moreover, FAST J0139+4328 ($l = 132°.097$, $b = -18°.548$) is away from the Galactic disk and nearly located in the direction of the anti-Galactic center. Using a new 3D map of dust reddening (Green et al. 2019), we determined that the dust reddening of $E(B - V)$ is 0.08 in the region of FAST J0139+4328. Because of the smaller reddening, the lack of an optical counterpart for FAST J0139+4328 is also not due to interstellar extinction.

One reason for the lack of an optical counterpart is the detection limitation of the Pan-STARRS1 data we used. There is a B-band Tully–Fisher relation for spiral galaxies (Tully & Fisher 1977; Zwaan et al. 1995), which is the most commonly used method for determining galaxy distances of redshifts. For FAST J0139+4328, we use the relation $M_{\mathrm{BT}} = -7.27 \times \log_{10} W_{20}^c + 1.94$ for spiral galaxies (Tully & Pierce 2000). The line width is corrected for the inclination angle (i) as $W_{20}^c = W_{20}/\sin(i)$. According to the B-band TF relation, FAST J0139+4328 should have an M_{BT} of -13.0 ± 0.4 mag if it is a disk galaxy. Nevertheless, FAST J0139+4328 has no optical counterpart. Here we can give an upper limit apparent magnitude for FAST J0139+4328. Using the software SEXtractor (Bertin & Arnouts 1996) and a row-by-row and column-by-column method (Wu et al. 2002; Du et al. 2015), we created a new sky-background subtraction.

For the optically dark FAST J0139+4328, it needs to set a reasonable aperture diameter. For a very faint optical galaxy, the flux from the sky background dominates the measurement (Leisman et al. 2021). They suggested that it should use a much smaller aperture to measure the flux of a faint galaxy, in order to try to limit the contribution from the sky background. The expected D_{25} of FAST J0139+4328 is $21''$. We adopted $D_{25}/2$ ($\sim$1300 pixels) as an aperture diameter for FAST J0139+4328. From the newly subtracted-background g-band and r-band images, we measured that the 3σ detection thresholds are 21.7 mag (m_{r}) and 22.0 mag (m_{g}) in r band and g band for FAST 0134+5737, which are corrected for Galactic extinction by a new 3D map of dust reddening. Using the transformations for the measured magnitudes from the g band and r band to the B band, the upper limit apparent B-band magnitude can be determined by the equation $m_B = m_g + 0.47(m_g - m_r) + 0.17$ (Smith et al. 2002). Then we derived that the upper limit absolute B-band magnitude (M_B) is -10.0 mag, which is several magnitudes larger than that predicted by the B-band TF relation. It shows that if there is an optical counterpart in the dark galaxy FAST J0139+4328, the Pan-STARRS1 survey images should be able to reveal the optical emission of the counterpart.

To compare with other faint galaxies, we calculated the H I mass-to-light ratio (M_{HI}/L_B). The B-band luminosity can be determined by $L_B = D^2 10^{10 - 0.4(m_B - M_{B0})}$, where M_{B0} is the absolute solar B-band magnitude, which is adopted as 5.44 mag (Willmer 2018). Using the M_{II} of $(8.3 \pm 1.7) \times 10^7 M_{\odot}$, we obtained that M_{HI}/L_B is $\geqslant 59\ M_{\odot}/L_{\odot}$ for FAST J0139+4328, which is much higher than those of 0.15 to 4.2 found in more normal galaxies (Brunker et al. 2019). Figure 3(b) shows a relationship between M_{HI}/L_B and M_B. We see that FAST J0139+4328 is almost the darkest gas-rich galaxy. Furthermore, using the $g - r$ color value and B-band luminosity (Zhang et al. 2017), we estimated that the upper limit stellar mass of FAST J0139+4328 is $6.9 \times 10^5 M_{\odot}$. This is the first time that a gas-rich isolated dark galaxy has been detected in the nearby universe. In addition, a galaxy is assumed to form from gas, which cools and turns into stars at the center of a halo. FAST J0139+4328 has a rotating disk of gas and is dominated by dark matter, but is starless, implying that this dark galaxy may be in the earliest stage of galaxy formation. According to a prior model, however, most of the gas in dark galaxies with baryonic masses greater than $10^9\ M_{\odot}$ will inevitably become Toomre unstable and give rise to star formation in the absence of an internal radiation field (Taylor & Webster 2005). We calculated the baryonic mass of FAST J0139+4328 to be $(1.1 \pm 0.3) \times 10^8 M_{\odot}$, indicating that this dark galaxy can endure for a considerable amount of time before being discovered. As a result, we can now detect this dark galaxy. Future blind H I surveys with high sensitivity and high-velocity resolution are expected to contribute considerably to our understanding of the absence of ultra-faint galaxies.

ORCID iDs

Jin-Long Xu https://orcid.org/0000-0002-7384-797X
Ming Zhu https://orcid.org/0000-0001-6083-956X
Naiping Yu https://orcid.org/0000-0003-1241-7439
Chuan-Peng Zhang https://orcid.org/0000-0002-4428-3183
Xiao-Lan Liu https://orcid.org/0000-0002-1768-9591

References

Ball, C., Cannon, J. M., Leisman, L., et al. 2018, AJ, 155, 65
Behroozi, P. S., Marchesini, D., Wechsler, R. H., et al. 2013, ApJL, 777, L10
Bertin, E., & Arnouts, S. 1996, AAS, 117, 393
Broeils, A. H., & Rhee, M. H. 1997, A&A, 324, 877
Brunker, S. W., McQuinn, K. B. W., Salzer, J. J., et al. 2019, AJ, 157, 76
Bullock, J. S., & Boylan-Kolchin, M. 2017, ARA&A, 55, 343
Cannon, J. M., Martinkus, C. P., Leisman, L., et al. 2015, AJ, 149, 72
Chambers, K. C., Magnier, E. A., Metcalfe, N., et al. 2016, arXiv:1612.05560
Davies, J. I., Disney, M. J., Minchin, R. F., et al. 2006, MNRAS, 368, 1479
Doyle, M. T., Drinkwater, M. J., Rohde, D. J., et al. 2005, MNRAS, 361, 34
Du, W., Wu, H., Lam, M. I., et al. 2015, AJ, 149, 199
Duc, P. A., & Bournaud, F,. 2008, AJ, 673, 787
Gaia Collaboration, Prusti, T., de Bruijne, J. H. J., et al. 2016, A&A, 595, A1
Glowacki, M., Collier, J. D., Kazemi-Moridanl, A., et al. 2022, ApJ, 931, L7
Green, G. M., Schlafly, E., Zucker, C., et al. 2019, ApJ, 887, 93
Haynes, M. P., Giovanelli, R., Martin, A. M., et al. 2011, AJ, 142, 170
Hess, K. M., Roberts, H., Dénes, H., et al. 2021, A&A, 647, 193
Hoffman, G. L., Salpeter, E. E., Farhat, B., et al. 1996, ApJS, 105, 269
Honey, M., van Driel, W., Das, M., & Martin, J. M. 2018, MNRAS, 476, 4488
Janowiecki, S., Leisman, L., Józsa, G., et al. 2015, ApJ, 801, 96
Jiang, P., Tang, N.-Y., Hou, L.-G., et al. 2020, RAA, 20, 064
Jiang, P., Yue, Y. L., Gan, H. Q., et al. 2019, SCPMA, 62, 959502
Józsa, G. I. G., Kenn, F., Klein, U., & Oosterloo, T. A. 2007, A&A, 468, 731
Kauffmann, G., White, S. D. M., & Guiderdoni, B. 1993, MNRAS, 264, 201
Kourkchi, E., Courtois, H. M., Graziani, R., et al. 2020, AJ, 159, 67

Leisman, L., Haynes, M. P., Janowiecki, S., et al. 2017, ApJ, 842, 133
Leisman, L., Rhode, K. L., Ball, C., et al. 2021, AJ, 162, 274
Martin, D. C., Fanson, J., Schiminovich, D., et al. 2005, ApJ, 619, L1
McGaugh, S. S. 2012, AJ, 143, 40
Moore, B., Ghigna, S., Governato, F., et al. 1999, ApJ, 524, L19
Roman, J., Jones, M. G., Montes, M., et al. 2021, A&A, 649, L14
Sales, L. V., Wetzel, A., & Fattahi, A. 2022, NatAs, 6, 897
Sawala, T., Frenk, C. S., Fattahi, A., et al. 2016, MNRAS, 457, 1931
Skrutskie, M. F., Cutri, R. M., Stiening, R., et al. 2006, AJ, 131, 1163
Smith, J. A., Tucker, D. L., Kent, S., et al. 2002, AJ, 123, 2121
Solanes, J. M., Giovanelli, R., & Haynes, M. P. 1996, ApJ, 461, 609
Taylor, E. N., & Webster, R. L. 2005, ApJ, 634, 1067
Taylor, R., Davies, J. I., Jáchym, P., et al. 2016, MNRAS, 461, 3001
Taylor, R., Davies, J. I., Jáchym, P., et al. 2017, MNRAS, 467, 3648
Tollerud, E. J., Bullock, J. S., Strigari, L. E., & Willman, B. 2008, ApJ, 688, 277
Toribio, M. C., Solanes, J. M., Giovanelli, R., et al. 2011, ApJ, 732, 93
Tully, R. B., & Fisher, J. R. 1977, A&A, 54, 661
Tully, R. B., & Pierce, M. J. 2000, ApJ, 533, 744
Turner, N. J. J., & MacFadyen, A. A. 1997, MNRAS, 285, 125
Westmeier, T., Jurek, R., Obreschkow, D., et al. 2014, MNRAS, 438, 1176
Willmer, C. N. A. 2018, ApJS, 236, 47
Wu, H., Burstein, D., Deng, Z. G., et al. 2002, AJ, 123, 1365
Xu, J. L., Zhang, C. P., Yu, N., et al. 2021, ApJ, 922, 53
Zhang, C. P., Xu, J. L., Li, G., et al. 2021, RAA, 21, 209
Zhang, C. P., Xu, J. L., Wang, J., et al. 2022, RAA, 22, 025015
Zhang, H. X., Puzia, T., & Weisz, D. R. 2017, ApJS, 233, 12
Zhang, J. S., Wang, J. Z., Di, G. X., et al. 2014, A&A, 570, A110
Zwaan, M. A., van der Hulst, J. M., de Blok, W. J. G., & McGaugh, S. S. 1995, MNRAS, 273, L35